Environmental aging effects on high performance biocomposites reinforced by sisal fibers

Bernardo Zuccarello*, Carmelo Militello, Francesco Bongiorno

Department of Engineering, University of Palermo, Viale delle Scienze, 90128 Palermo

Corresponding author, e-mail: bernardo.zuccarello@unipa.it

Abstract

Among the innovative materials, an important role is played by the so-called *biocomposites*, generally made by an eco-friendly matrix reinforced with natural fibers. Unfortunately, due to the more degradability of the green matrix as well as to hydrophilicity of the natural fiber, the resistance of such innovative materials to the environmental agents is in general relativity low, and it can significantly limit their use in outdoor conditions. In order to give a contribution to the knowledge of the effects of the main environmental agents on the mechanical properties of high-performance biocomposites made of green epoxy matrix reinforced by agave fibres, a systematic experimental testing campaign has been carried out by considering three types of biocomposite laminates that can be use for structural applications (unidirectional, cross-ply and quasi-isotropic with a V_f = 70%), has been considered. In order to highlight the different effects of aging on matrix and reinforcement, samples consisting of simple epoxy matrix alone have been analysed too. In order to reproduce the usual operating conditions associated with periodic exposure to sunlight (temperature and UV cycles) and humidity related to external environmental conditions, all the materials considered have been subjected to an accelerated aging process in accordance with the ASTM G 154 standard. The analysis of the experimental results was also aimed to the developing of reliable models that can be used to predict the degradation of the main mechanical properties of these materials, when they are subjected to the actual aging related to the outdoor service conditions.

Keywords: Biocomposites, Sisal fiber, B. Environmental degradation, B. Mechanical properties.

1. INTRODUCTION

The increasing interest in protecting the environment has led to a significant focus on the effects of pollution associated with the production and end-of-life disposal of technical materials, such as metals and synthetic

materials, responsible for significant CO_2 emissions. Consequently, biocomposites, consisting of low environmental impact matrices reinforced by natural fibers, are an attractive alternative to traditional materials. In particular, biocomposites have in general specific properties comparable or superior to those of technical metals, such as steel and aluminum, and some synthetic composites, especially those reinforced by glass fibers.

In more detail, the low cost and high availability of sisal fibers in the current market, make their high performance biocomposites, an interesting alternative to synthetic composites for a variety of semi-structural and structural applications, in addition to the common applications, already very diffuse, related to the production of internal parts and components in the automotive sector [1,2], boating and civil construction. Such innovative materials have so far been poorly used in outdoor environments, especially under harsh environmental conditions, as few studies on the durability of these materials are yet available.

Despite the mitigating presence of the hydrophobic matrixes, the hydrophilic nature of plant fibers implies the easy absorption of moisture from the surrounding environment with presumably weakening of the fiber as well as of the fiber-matrix adhesions, with consequent significant reduction of the mechanical properties of the biocomposites [3–6].

In [7] has been performed a careful comparison of the bio-properties hybrid of and pure biocomposites reinforced with kenaf and sisal fibers, used for semi-structural applications in the construction sector; the analysis of the main mechanical properties before and after aging tests has shown that hybridization results in a significant reduction in durability.

In [8], the mechanical properties of both fresh and aged sisal fiber-reinforced polypropylene-based composites were evaluated. The results showed that composite with aged fibers shows better mechanical properties than fresh fiber composites. The proposed reason is that the mechanical properties of composites are not only based on the strength of the fiber alone, which is better in the fresh fiber, but also on the interfacial adhesion between the fiber and the matrix that favors the needed transfer of stresses.

Several works are found in literature on the effect of aging in biocomposites reinforced with flax fibers. As an example, in [9], Moudood et al. correlated moisture absorption to the physical changes and mechanical properties of bio-epoxy composites reinforced by flax fibre. They considered the cycle from material production to saturation by immersion in water, a decrease in tensile strength and stiffness by 9% and 57% respectively.

In [10], after a preliminary evaluation of the possibility of using natural fibres such as flax, coconut and basalt for the reinforcement of bio-polyethylene, the influence of aging on the mechanical properties of the biocomposites thus obtained was also evaluated.

In [11], an interesting study was presented to evaluate the temporal evolution of the mechanical performance of an epoxy composite reinforced by flax fibres exposed to wet/dry cycles for 104 consecutive days. The authors have shown, in particular, that the treatment of fibers leads to a better durability of the composite.

In [12] the authors showed how treatments on natural fibers influence the performance and durability of their composites. Composites prepared from jute fiber treated with a low concentration alkaline solution, exhibited improved mechanical properties and thermal stability. They also showed lower photoresistance and bioaccessibility/bio-disintegration.

In [13], the authors explored the weathering effects on of high density polyethylene composites with different biofiber fillers and coupling agent. The flexural strength and impact properties of samples exposed to weathering are decreased in application by the type of fiber or coupling agent. Woody fiber can be substituted with alternate biofibers such as cotton burr with stem and guayule bagasse with some variations in the physico-mechanical properties of the resultant composites.

Synergistic effects involved in the environmental degradation of Glass Reinforced Polymer (GRP) composites were examined in [14]. Six GRPs based on E-glass and ECR-glass fibers with four different polymer resins were exposed either individually or in combination to ultraviolet (UV) radiation, water condensation and elevated temperature for approximately 1000 h. It has been shown that the selected aging conditions load to noticeable synergistic effects, causing extensive erosion of the polymer matrices of the tested composites which appeared to be much stronger under the combined actions than under individual exposures.

The same authors in [15] clearly explained why the degradation of polymers and fiberglass from exposure to UV rays in the presence of occasional slow flows of water is much faster than simple UV rays. Furthermore, they have shown that UV damage on irregular polymer surfaces reduce their surface roughness making them planar and that the degradation rates are the greatest at the peaks of the local surface heights [16].

In [17], the authors have developed a novel in-situ aging evaluation system to simulate natural weathering, and the sensitivity was further improved. Through the reconstruction of the in-situ reaction cell, the seal performance was obviously improved.

In order to give a further contribution to the knowledge of the effects of the environmental aging on biocomposites, this work, intends to investigate the influence of environmental aging on the mechanical properties of high-performance biocomposites consisting of a "green epoxy" matrix reinforced with sisal fibers. These biocomposites have already been developed by the same authors [18,19,28–31,20–27]by means of preliminary manual packaging of unidirectional “stitched” fabrics, successive hand lay-up of the laminate, and subsequent compression molding

process. As widely demonstrated in [19-21, 23], .such biocomposites can be used advantageously to substitute metals and synthetical fiber composites in many practical application.

2. MATERIALS

In the following, after a brief description of the mechanical properties of the fibers and of the matrix used for the manufacturing of the considered high performance biocomposites reinforced by sisal fibers, three different laminates (unidirectional, cross-ply and quasi-isotropic, each with V_f=0.70) have been considered in order to obtain sufficient information to describe the environmental aging effects on a generic angle-ply laminate used in practice for structural and semi-structural applications.

2.1 Matrix and fibers

The high performance biocomposites considered, are constituted by a green epoxy resin (partial biobased epoxy) produced by the American Entropy Resin Inc. (San Antonio, CA, USA), called SUPERSAP CNR, with IHN type hardener. As widely shown in previous studies [18–25] carried out by the same authors, this matrix exhibits an almost linear elastic behaviour, with the following main characteristics: density ρ_m = 1.05 g/cm^3, tensile strength $\sigma_{m,R}$ = 60 MPa, Young's modulus E_m = 2.5 GPa, and tensile stress strain $\varepsilon_{m,R}$ = 2.5%.

The fibers used as reinforcement are sisalane agave fibers (sisal), specially extracted from the middle third of mature leaves, selecting in particular the perimeter ones (structural fibers) which exhibits the best mechanical properties. In order to maintain a high degree of renewability, the fibers were subjected only to a manual cleaning process and subsequent drying, without any surface treatment with caustic soda or other similar detergent. The main mechanical properties of the batch of fibers actually used in the present work, were evaluated by means of specific tensile tests on a single fiber; the following mean results were obtained: tensile strength $\sigma_{f,R}$ = 690 MPa, longitudinal Young's modulus E_f = 40 GPa and failure tensile strain $\varepsilon_{f,R}$ = 1.7% (standard deviation of 6-8% have been obtained by using a sample of 10 fibers).

2.2 Manufacturing of the laminates

High-quality stitched fabrics were preliminarily made in laboratory by a relatively laborious process consisting of: (a) manual stretching of the fiber in order to eliminate the natural undulations, (b) alignment of the rectilinear fibers arranged in small groups and (c) cross stitching with a special automatic sewing machine. In this way, unidirectional fabrics with a specific weight of about 240 g/m^2 were obtained (see Fig.1).

Figure 1 Unidirectional sisal stitched fabrics properly made in the laboratory.

The manufacturing of the various laminates was carried out by hand lay-up performed on a suitable square mould of 260x260 mm (Fig.2a). To obtain good quality laminates, after an appropriate period of partial gelling of the matrix, carried out in accordance with the optimal process described in [20,21], the laminates were subjected to a compression-moulding process, using a 100-ton press (Fig.2b) for 24 hours. In order to optimize the mechanical characteristics, each laminate was subjected to a subsequent cure at a temperature of 80 °C for 5h.

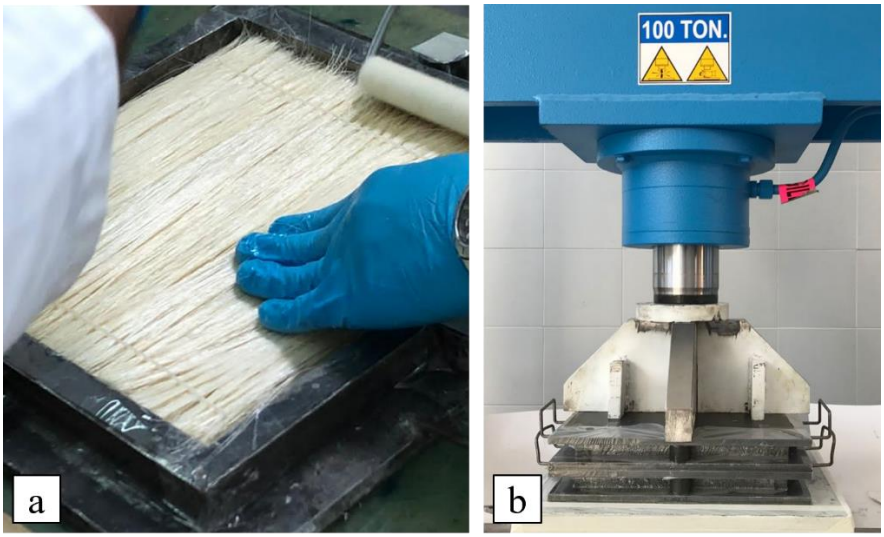

Figure 2 Biocomposite manufacturing: (a) hand lay-up inside the mould, (b) compression moulding by 100 tons hydraulic press.

In this way, three different biocomposite laminates consisting of 16 oriented laminae, with a volume percentage of reinforcement V_f =70% and a thickness of about 3.8 mm, have been manufactured. In detail, a unidirectional laminate $[0_8]_S$, a cross-ply laminate $[(0/90)_4]_S$ and a quasi-isotropic $[(0/\pm45/90)_2]_S$ were made. In addition, a neat resin panel was also manufactured in order to evaluate the effects of aging on the matrix alone, and so to estimate the contribution of the aging due to fibers, by comparing the aging of biocomposites with the aging of the matrix

alone. From each biocomposite laminate so obtained, rectangular samples with dimensions congruent with those of the sample holder system that equips the accelerated aging machine, have been cut with a proper dish mill.

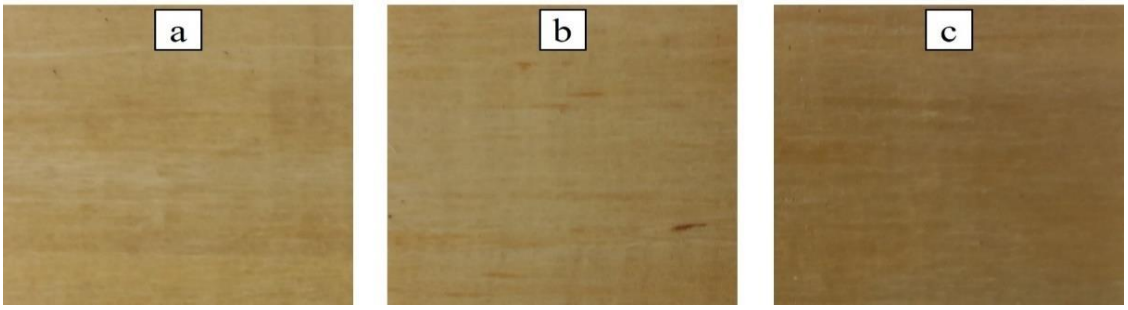

Figure 3 Laminate biocomposite considered: (a) unidirectional laminate [08]S, (b) cross-ply laminate [(0/90)4]S and (c) quasi-isotropic [(0/±45/90)2]S.

3. EXPERIMETAL TEST METHODS

The biocomposites samples have been subjected to an accelerated aging process with controlled conditions of temperature, humidity and UV radiation, that allow in practice to reproduce environmental effects such as exposure to sunlight and humidity from rain and dew. Static mechanical tests were performed to evaluate the influence of such accelerated aging on the main mechanical properties of the laminates considered.

3.1 Accelerated aging

The biocomposite samples were exposed to cycles of UV radiation (UVA-340) and water condensation using a QUV-type accelerated aging machine (see Fig.4a). In more detail, Alternating cycles of UVA radiation (8 h) at 70 °C and water condensation (4 h) at 50 °C were applied, for a period of 8 weeks (56 days, 1344 h). The tests have been carried out in accordance with ASTM G 154 [32] (standard used for aging equipment in fluorescent light for UV exposure of non-metallic materials). Rectangular specimens having dimensions of 80x160 mm have been placed in a special specimen rack (see Fig.4b) situated inside the aging chamber. Every 2 weeks (336 h) a sample was taken for each material analysed (resin and three different biocomposite laminates), for a total of four overall samples, made after 2 (336 h), 4 (672 h), 6 (1008 h) and 8 (1344 h) weeks.

Figure 4 (a) QUV-accelerated weathering tester; (b) specimen rack placed into the aging chamber.

3.2 Tensile test

The effects of environmental aging on the mechanical properties of the biocomposites laminates have been evaluated through special tensile tests. These tests were carried out both on the materials immediately after their production (virgin material), and after 2, 4, 6 and 8 weeks of accelerated aging, in accordance with the set aging program. An MTS 793 servo-hydraulic machine, instrumented with a extensometer with a 25 mm measuring base, was used for the tensile tests (see Fig.5a) carried out in accordance with the ASTM D3039 standard [33] (for each materials three rectangular specimens having dimensions of 25 x160 mm, were tested).

3.3 ILSS test

The effects of the weathering on the matrix and on the fiber-matrix interface, have been evaluated by interlaminar shear strength (ILSS) tests carried out, in accordance with the ASTM D2344 standard [34]. The tests were carried out at a test speed of 1 mm / min using the same MTS 793 servo-hydraulic machine (see Fig.5b). In accordance with the aforementioned standard, three rectangular specimens having dimension of 8 mm x 25 mm 3.8 mm (short beam) was placed on two supports having a spun equal to about four times the thickness of the specimen itself (4 x 3.8 ≈15 mm) and loaded in three-point bending.

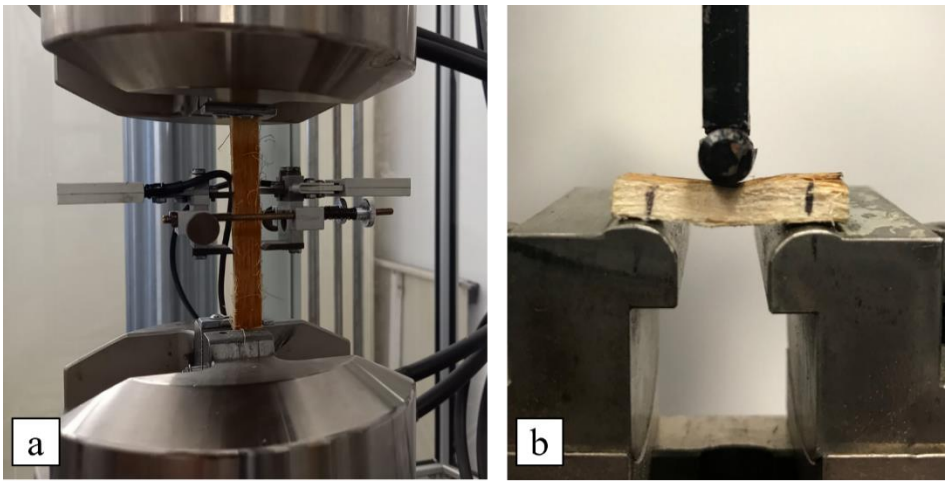

Figure 5 Testing of biocomposite specimens: (a) Tensile test and (b) ILSS test.

4. EXPERIMENTAL RESULTS

The results of the mechanical tests carried out on virgin materials and on the same materials after accelerated aging are reported below, after a preliminary visual analysis of the exposed surfaces.

4.1 Visual analysis

From the following Fig.6, which shows the images of the specimens of the different materials after successive aging periods, it is first of all possible to note how the cyclic accelerated aging process used in this work produces

an appreciable colour variation on the external surface of the specimens, with progressive yellowing that, from an initial light-yellow colour, leads to an increasingly intense brown tint.

Figure 6 Specimens subjected to different accelerated aging steps.

As can be seen from the evolution of the surface aging of the neat resin specimens, these colour variations effects are essentially linked to the aging of the resin, being relatively limited the contribution due to the aging of the underneath fibers and to a lesser extent to the aging of the fiber.

4.2 Tensile strength

The following figures (Fig.7a, 8a, 9a and 10a) show the graphs of the average tensile curves obtained for the various materials analysed, considering the virgin materials (0 weeks) and the 4 distinct conditions of progressive aging (2, 4, 6, 8 weeks). The experimental results of the various tests performed, are generally characterized by an average scattering corresponding to a standard deviation in the range 3-5%.

4.2.1 Green epoxy resin

From the analysis of the curves relating to the neat resin (Fig.7) it can be seen how the exposure to the accelerated aging process for a time of 2 weeks (336 hours) gives rise to an embrittlement of the material with an approximately halving of the failure strain (from about 3% to about 1.5%) and associated significant reduction in tensile strength of about 30% (from about 60 MPa to about 43 MPa).

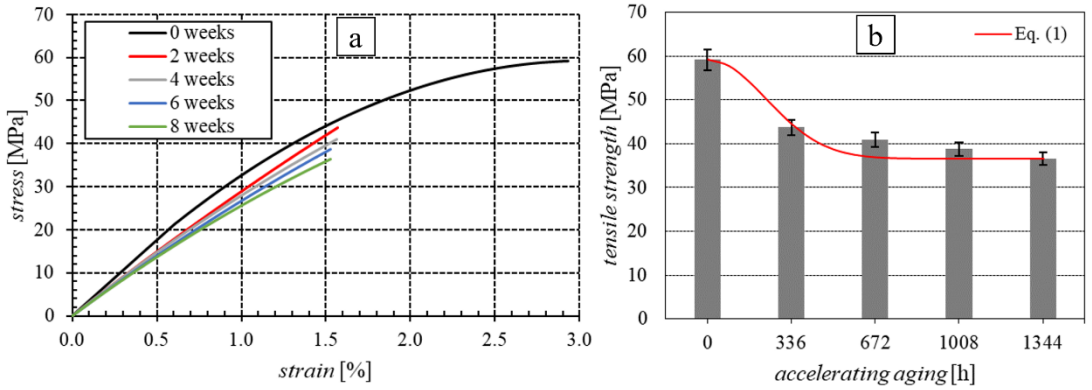

Figure 7 (a) Mean tensile stress curves of the various specimens with neat epoxy and (b) tensile strength after the progressive aging.

On the other hand, the aging effects on the Young's tensile modulus of the green epoxy are relatively small (reduction of about 10%). In more details, aging leads to more linear curve: the matrix loses the initial well known partial plasticity, which gives rise to a slight reduction of the epoxy stiffness as the applied load increases. For accelerated aging values greater than 2 weeks of exposure (336 h), significant variations in the failure strain are no longer observed but only further (relatively limited) reductions in tensile strength are observed, which reaches the minimum value of about 36 MPa after 8 weeks of aging (1344 h). In summary, it is possible to state that the accelerated aging gives rise to a degradation of the tensile performance, characterized by an asymptotic trend with an initial phase (first 2 weeks approximately) in which there is an average tensile strength percentage reduction of the order of approximately 1%, for every 10 hours of accelerated aging, followed by a second phase (from 2 to 8 weeks) much slower and characterized by an average reduction of about 2% for every 100 hours (see Fig.7); after about 8 weeks such reduction became negligible and the overall reduction of the tensile strength reach the value of about 40%; also, it is associated with an overall stiffness decrease of about 18%. Synthetically, unlike expected for thin specimens for which the aging involves in practice the uniform degradation of the mechanical property that tend to zero when *t* tend to infinite, for the examined specimens having thickness relatively high (about 4 mm), the aging involves in practice only the surface and the subsurface material, without appreciable effects on the internal material; consequently, the degradation process of the specimens is not represented by a classical asymptotical function that tends to zero, but it tends to a finite value. In other words, after 8 weeks of accelerated aging the surface/subsurface materials in practice is completely aged whereas the internal material continues to be protected by the environmental agents by the same aged surface/subsurface materials. For these reasons, the analysis of the degradation of the tensile strength S_R^{GE} of the green epoxy resin, shows how this phenomenon obeys in practice to an approximated exponential aging law, represented in practice by the following formula:

$$S_R^{GE}(t) = [S_R^{GE}(0\ h) - S_R^{GE}(1344\ h)]e^{-k_{ACC}^{GE}\,t^2} + S_R^{GE}(1344\ h) \qquad (1)$$

being k_{ACC}^{GE} = 9.35 x 10^{-6} the constant of the exponential law that governs the rate of degradation, $S_R^{GE}(0h)$ = 60 MPa and $S_R^{GE}(1344\ h)$= 36 MPa respectively the tensile strength of the virgin resin and of the resin subjected to an accelerated aging for *t*= 1344 h; the apexes *GE* and *ACC* means respectively *Green Epoxy* and *Accelerated Aging*. As it can be seen from Fig.7b, this relationship interpolates the experimental data with an uncertainty generally lower than 7-8%. Obviously, Eq.1 can be advantageously used at the design stage to evaluate the degradation of the tensile strength corresponding to the exposure to the accelerated aging considered, for a generic design time *t*.

4.2.2 Unidirectional biocomposite (UD)

Considering the unidirectional biocomposite (UD), from the following Fig.8a, that shows the curves of the corresponding tensile tests, it can be observed that unlike neat resin, the accelerated aging of the biocomposite does not lead to significant variations in the failure strain, which is always kept around 1.75%, that is in practice the failure strain of the sisal fibers considered. Obviously, this effect is closely linked to the presence of fibers, so it can be said that the accelerated aging does not lead to appreciable variations of the failure strain of the analysed biocomposites. On the other hand, an appreciable progressive reduction of the stiffness is observed, with loss of the initial linearity of the biocomposite (effects probably linked to the aging of the fibers and/or of the resin/fiber interface) associated with a significant comparable reduction of the failure strength.

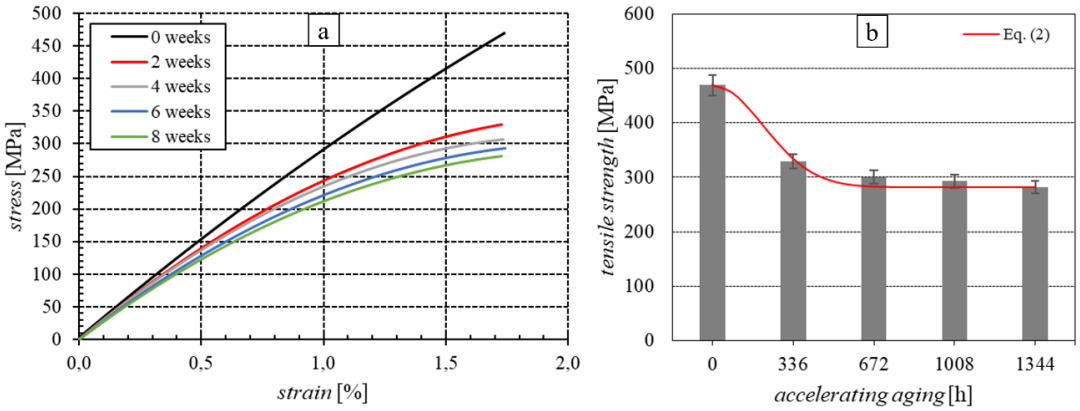

Figure 8 (a) Mean tensile stress curves of the unidirectional specimens subjected to various accelereted aging, and (b) corresponding tensile strength after the progressive aging.

In more detail, it can be said that a first phase (up to about 350 h), characterized by a fast relative aging that leads to a reduction of both strength and average stiffness of about 30%, is observed; it is followed by a second phase (up to about 1344 h), characterized by a slower aging that leads to a further loss of strength and stiffness of about 10% or less. After 1344 h of accelerated aging, a strength reduction of about 40% (comparable with that of the neat resin) with an associated reduction of about -40% of the average stiffness higher than the value of the -18% of the neat resin), is observed. Also in this case, as it can be seen from Fig.8b, the degradation of the longitudinal

tensile strength $S_{L,R}^{UD}$ (in the direction of the fibers) of the unidirectional biocomposite is well approximated by the function represented by Eq.1, which takes the following expression:

$$S_{L,R}^{UD}(t) = \left[S_{L,R}^{UD}(0\ h) - S_{L,R}^{UD}(1344\ h)\right]e^{-k_{ACC}^{UD}\,t^2} + S_{L,R}^{UD}(1344\ h) \quad (2)$$

being in this case k_{ACC}^{UD}=1.12 x 10^{-5}, $S_{L,R}^{UD}(0\ h)$ = 469 MPa (tensile strength of the virgin UD biocomposite) and $S_{L,R}^{UD}(1344\ h)$= 281 MPa (tensile strength of the UD biocomposite completely aged).

4.2.3 Cross-ply biocomposite (CP)

Furthermore, considering the cross-ply biocomposite (CP), from the following Fig.9a it is seen how the aging produces also in this case appreciable stiffness reductions of the biocomposite (due to the aging of the fibers and/or the interface), along with a comparable reduction of the failure strength. Regarding the progression of the effects of aging with the exposure time, also in this case it is observed a first phase (up to about 300 h) which is characterized by relatively fast reduction a reduction in strength and stiffness of about 25% (more modest than the UD), followed by a second phase (up to about 1344 h) characterized by a much slower aging that leads to a further loss of strength and stiffness of about 10% (as for the UD). In this case after 1344 h of accelerated aging there is, therefore, an overall reduction in strength, equal to about 35%, slightly lower than that of the neat resin and of the unidirectional biocomposite (40%). Also, in this case the stiffness undergoes a progressive reduction with the load, starting from the value of the virgin material for low loads. Also, as it can be seen from Fig.9b, for the cross-ply biocomposite, the degradation of the tensile strength is well approximated by Eq.3:

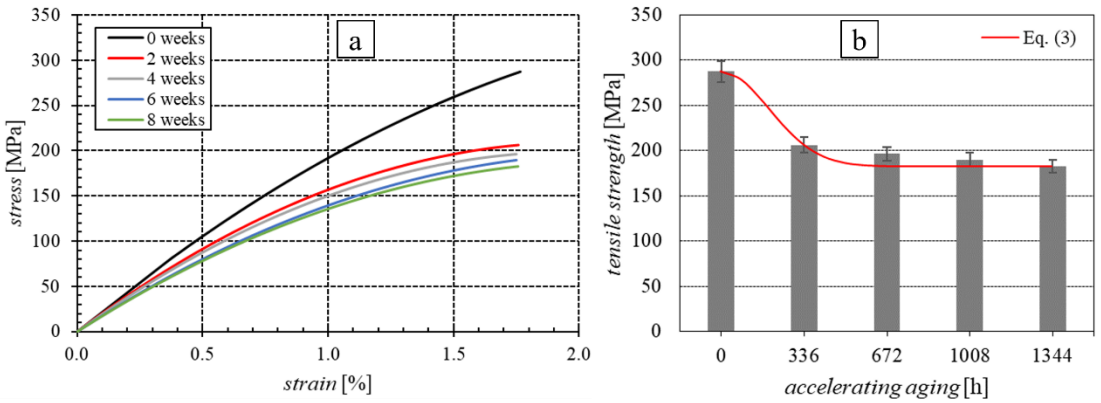

Figure 9 (a) Mean tensile stress curves of the cross-ply specimens subjected to various accelereted aging, and (b) corresponding tensile strength after the progressive aging.

$$S_{L,R}^{CP}(t) = \left[S_{L,R}^{CP}(0\ h) - S_{L,R}^{CP}(1344\ h)\right]e^{-k_{ACC}^{CP}\,t^2} + S_{L,R}^{CP}(1344\ h) \quad (3)$$

whit k_{ACC}^{CP}=1.30 x 10^{-5}, $S_{L,R}^{CP}(0\ h)$ =287 MPa and $S_{L,R}^{CP}(1344\ h)$=182 MPa.

4.2.4 Quasi-isotropic biocomposite (QI)

Finally, considering the quasi-isotropic biocomposite (QI), from the following Fig.10a it is observed that, also in this case, the aging leads to an appreciable reduction in stiffness with associated reduction in failure strength (mainly due to the aging of the fibers).

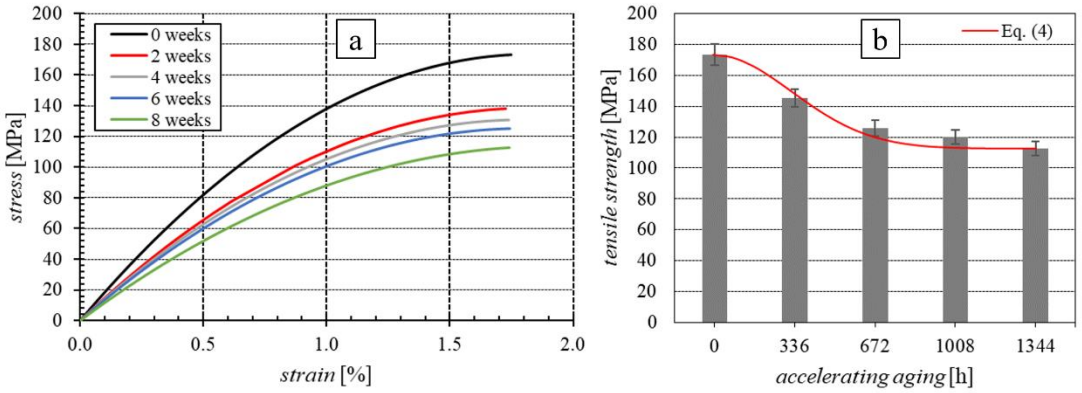

Figure 10 (a) Mean tensile stress curves of the various quasi-isotropic specimens and (b) tensile strength after the progressive aging.

Also, in this case a faster first phase is observed which leads to a degradation of stiffness and strength of about 19% after about 300 h, followed by a further reduction of about 15%, that lead to an overall environmental degradation of 34% about. These effects are therefore completely comparable with those of the CP biocomposite, both slightly lower than that of the UD biocomposite. Also in this case, as it can be seen from Fig.10b, the degradation of the longitudinal tensile strength $S_{L,R}^{QI}$ (in the direction of the fibers of the surface laminae) of the quasi-isotropic biocomposite is well approximated by Eq.4:

$$S_{L,R}^{QI}(t) = \left[S_{L,R}^{QI}(0\ h) - S_{L,R}^{QI}(1344\ h)\right]e^{-k_{ACC}^{QI}\,t^2} + S_{L,R}^{QI}(1344\ h) \qquad (4)$$

with k_{ACC}^{QI} = 4.65 x 10^{-6}, $S_{L,R}^{QI}(0h)$ = 173 MPa and $S_{L,R}^{QI}(1344\ h)$= 113 MPa.

4.2.5 Percentage degradation and prediction of the aging evolution under service conditions

Taking into account that, as above observed experimentally, the aging of the examined biocomposite laminates, move always from the "virgin material" condition to the asymptotic condition of "completely aged material" condition, it follows that the corresponding degradation of the mechanical properties can be more advantageously represented in terms of percentage reduction relative to the value of the virgin material. As an example, the percentage reduction $\Delta S_{L,R}^{XY}\%_{ACC}(t)$ of the tensile strength of a generic *XY* laminate under the accelerated aging, can be expressed by the following formula derived directly from the above reported Eqs.2-4:

$$\Delta S_{L,R}^{XY}\%_{ACC}(t) = 100\left[1 - \frac{S_{L,R\ ACC}^{XY}(1344\ h)}{S_{L,R}^{XY}(0\ h)}\right](1 - e^{-k_{ACC}^{XY}t^2}) \qquad (XY = UD, CP \text{ and } QI) \qquad (5)$$

The constancy of the failure strain for any aging exposure time, observed experimentally above, leads to the fact that a similar formula gives also the percentage degradation of the mean Young modulus's at the incipient failure conditions, i.e. :

$$\Delta E_{L,R}^{XY}\%_{ACC}(t) = 100\left[1 - \frac{E_{L,R\ ACC}^{XY}(1344\ h)}{E_{L,R}^{XY}(0\ h)}\right](1 - e^{-k_{ACC}^{XY}t^2}) \qquad (XY = UD, CP \text{ and } QI) \qquad (6)$$

being $E_{L,R}^{XY}$ the mean Young modulus's corresponding to $\varepsilon = \varepsilon_{f,R} \simeq 1.75\%$.

Obviously, the k_{ACC}^{XY} exponent involved into Eq.5 and 6 depends on the material properties (it is in fact different for UD, CP and QI examined laminates), as well as on the peculiar characteristics of the aging process (severity of the environmental condition etc.). The values of k_{ACC}^{XY} for the three biocomposites laminates examined, have been reported in the following Tab.1, along with the values of $S_{L,R}^{XY}(0\ h)$, $E_{L,R}^{XY}(0\ h)$, $S_{L,R\ ACC}^{XY}(1344\ h), E_{L,R\ ACC}^{XY}(1344\ h)$ necessary to describe completely the behaviour of each material under accelerated aging.

Table 1 Characteristic values of the law of degradation for the biocomposites considered.

Material	$\boldsymbol{S_{L,R}(0\ h)}$ [MPa]	$\boldsymbol{S_{L,R\ ACC}(1344\ h)}$ [MPa]	$\boldsymbol{E_L(0\ h)}$ [GPa]	$\boldsymbol{E_{L,R\ ACC}(1344\ h)}$ [GPa]	$\boldsymbol{k_{ACC}^{XY}}$ [s^{-2}]
UD	469	281	27.1	16.1	1.12×10^{-5}
CP	287	182	16.4	10.4	1.30×10^{-5}
QI	173	113	9.9	6.5	4.65×10^{-6}

Obviously, the exposition to generic aging process related to the actual (*ACT*) service conditions lead to an actual percentage degradation $\Delta S_{L,R}^{XY}\%_{ACT}(t)$ included always between the same two extreme values corresponding to the initial virgin condition ($t = 0\ h$) and the final complete aged condition, already known by the accelerated aging above applied ($t = 1344\ h$), but it involves a different value of the exponent k_{ACT}^{XY}, i.e.:

$$\Delta S_{L,R}^{XY}\%_{ACT}(t) = 100\left[1 - \frac{S_{L,R\ ACC}^{XY}(1344\ h)}{S_{L,R}^{XY}(0\ h)}\right](1 - e^{-k_{ACT}^{XY}t^2}) \qquad (7)$$

Such an unknown exponent k_{ACT}^{XY} can be obtained through a simple calibration of the relative aging curve if the calibration value $\Delta S_{L,R}^{XY}\%_{ACT}(t^*)$ of the percentage reduction after a time exposure t^* is known. By using this, Eq.7 can be rewritten as:

$$\Delta S_{L,R}^{XY}\%_{ACT}(t^*) = 100\left[1 - \frac{S_{L,R\ ACC}^{XY}(1344\ h)}{S_{L,R}^{XY}(0\ h)}\right](1 - e^{-k_{ACT}^{XY}t^{*2}}) \qquad (8)$$

From Eq.8 the unknown value of constant k_{ACT}^{XY} relative to the actual aging process can be obtained immediately by the following calibration formula:

$$k_{ACT}^{XY} = -\frac{1}{(t^*)^2}\ln\left[1-\frac{\Delta S_{L,R}^{XY}\%_{ACT}(t^*)}{\Delta S_{L,R}^{XY}\%_{ACC}(t^*)}\right] \quad (9)$$

As an example, for a UD specimen positioned in an outdoor setting (near our laboratory), after a time t^*=21 weeks = 3528 hours, an actual percentage degradation of the tensile strength $\Delta S_{L,R}^{UD}\%_{ACT}(t^*) = 12\%$ has been relieved. Consequently, Eq.9 provides:

$$k_{ACT}^{UD} = -\frac{1}{(3528)^2}\ln\left[1-\frac{12\%}{40\%}\right] = 2.86 * 10^{-8} \quad (10)$$

It is seen how k_{ACT}^{UD} takes a value very lower than the $k_{ACC}^{UD} = 1.12 \cdot 10^{-5}$ relative to the accelerated aging (3 order of magnitude), indicating a very lower severity of the aging process considered, respect the accelerated aging above used.

By introducing the values of k_{ACT}^{UD} =$2.86 * 10^{-8}$ into Eq.7, along with the extreme values of $S_{L,R\ ACC}^{UD}(1344\ h) = 281$ MPa and $S_{L,R}^{UD}(0\ h) = 469$ MPa (see Tab.1), then the function that describes the actual aging curve of the UD biocomposite laminate, is obtained immediately:

$$\Delta S_{L,R}^{UD}\%_{ACT}(t) = 100\left[1-\frac{281}{469}\right](1-e^{-2.86*10^{-8}*t^2}) \quad (11)$$

Such a curve is reported in the following Fig.11 along with the curve corresponding to the accelerated aging (Eq.2):

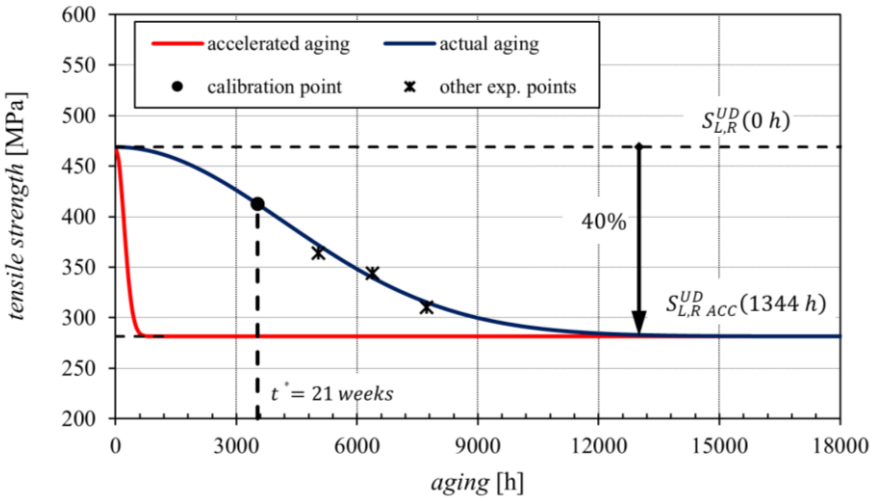

Figure 11 Comparison of the aging curves of the UD biocomposite laminate for accelerated aging and actual aging.

In order to assess the accuracy of the "actual aging" curve obtained by simple calibration, in the same Fig.11, other three points relieved experimentally, have been reported too.

Synthetically, from Fig.11 it is possible to observe how the calibration performed by using the accelerated aging results along with a calibration point, allows the user to obtain an accurate prediction of the "actual aging" curve relative to the aging due to a generic service conditions. In particular, such an approach permits to estimate the

time after which the analysed laminates reaches the asymptotical reduction of its performance (the tensile strength reduction of about 40%), that in this case is in practice equal to about 15÷18 thousand hours (about 2 years).

4.3 Delamination strength (ILSS test)

The following Fig.12 shows the average interlaminar shear strength (ILSS) values obtained experimentally in accordance with the ASTM D2344 [13] standard, for the various biocomposites analysed, considering for each material the condition of virgin material, with intermediate accelerated aging (2-6 weeks), and with complete accelerated aging (8 weeks).

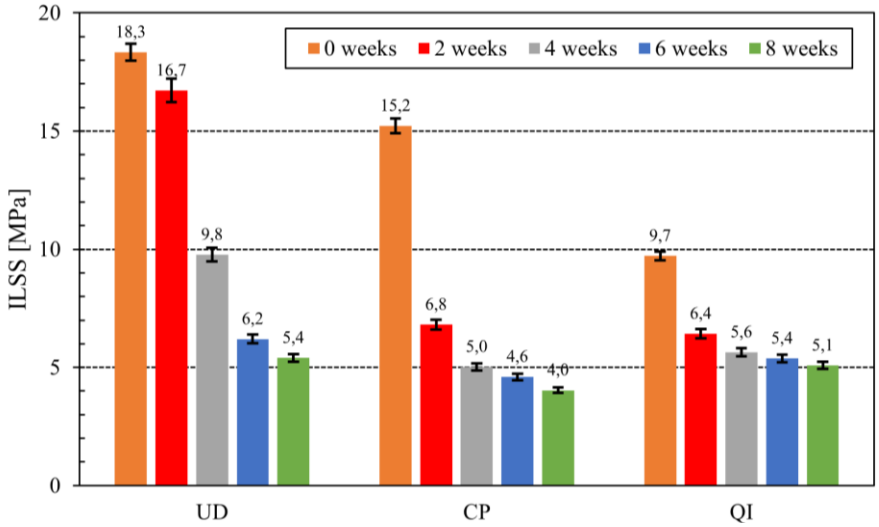

Figure 12 Results of the ILSS test for the different biocomposites analysed, after the progressive aging.

From the analysis of the results shown in Fig.12, it is possible to observe that the unidirectional biocomposite (UD), exhibits a reduction of the delamination strength, with an asymptotic decreasing trend. The exposure to 1344 hours of accelerated aging leads to a strength reduction approximately 70%, a value approximately double that already observed for the tensile test.

Considering the cross-ply biocomposite (CP), a more markedly asymptotic trend is observed which also leads to a significant reduction of the strength to delamination over time; in this case at the 1344 hours of exposure corresponds in practice a strength reduction of just over 70%, a value therefore comparable to that of the unidirectional biocomposites.

Finally, considering the quasi-isotropic biocomposite (QI), the decreasing asymptotic trend already seen for the previous cross-ply laminates is still observed, although with a more modest derivative than in the previous cases; at maximum aging corresponding to 1344 hours of exposure, it is now seen a percentage reduction of the delamination strength of approximately 50%, a value appreciably lower than that (70%) observed for the other biocomposite laminates.

From the processing of the results, a substantial difference was found between the ILSS values obtained from the tests performed with the aged surface of the specimens subjected to compressive loading, and that obtained with the aged surface subject to tensile loading. This difference was observed on all specimens, and it tends to increase with aging.

As an example, the following Fig.13 shows the average ILSS (*interlaminar shear strength*) values for the specimens subjected to 1008 and 1344 h of accelerated aging, respectively analysed according to the two test configurations, i.e. with the aged side subject to compressive (upper laminae of the specimen) and tensile (lower laminae of the specimen).

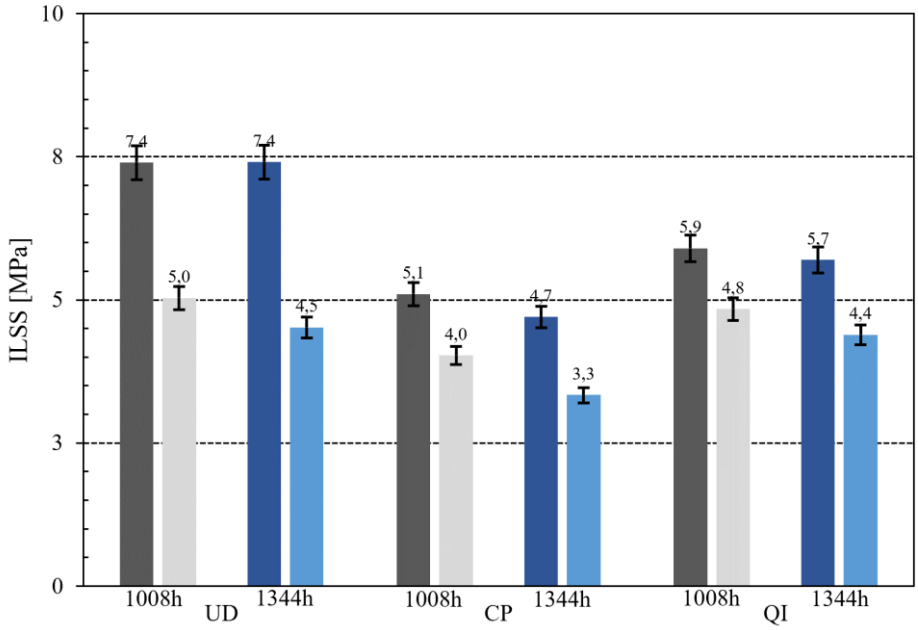

Figure 13 Average values ILSS for the various specimens subjected to 1008 and 1344 h of accelerated aging considering, with the aged side subject to compressive (upper laminae of the specimen) and tensile (lower laminae of the specimen).

From Fig.13 it is possible to observe how for all three types of laminates the strength to delamination is reduced more and more, when the aged side of the specimens is subjected to compressive. These reductions reach its maximum for the specimens subjected to 1344 hours of aging; in percentage terms, on average, a further reduction in strength to delamination of approximately 40%, 30% and 25% is observed for the UD, CP and QI laminate respectively. This reduction of delamination strength, when the specimen with the side exposed to aging is subjected to compressive load, is mainly due to the effects of "transverse tensile" on the matrix, due to the compressive loading, which obviously add up negatively to the effects of shear, by anticipating the delamination process. Therefore, it is possible to state that biocomposite laminates subject to primary bending loading stress are less resistant to delamination if the surface exposed to the environmental aging is subject to compressive. In the

design of laminates subjected to bending loading, it is therefore advisable, where possible, to expose to environmental agents the laminate surface subject to the tensile stresses.

5. DAMAGE MECHANISMS OF AGED BIOCOMPOSITE LAMINATES

The following Fig.14 shows the damage due to the tensile test on UD, CP and QI specimens completely aged, i.e. subjected to an accelerated aging of 8 weeks (1344 *h*) . The images of the partially aged specimens are omitted as they have practically shown the same damage mechanisms as the fully aged specimens shown here.

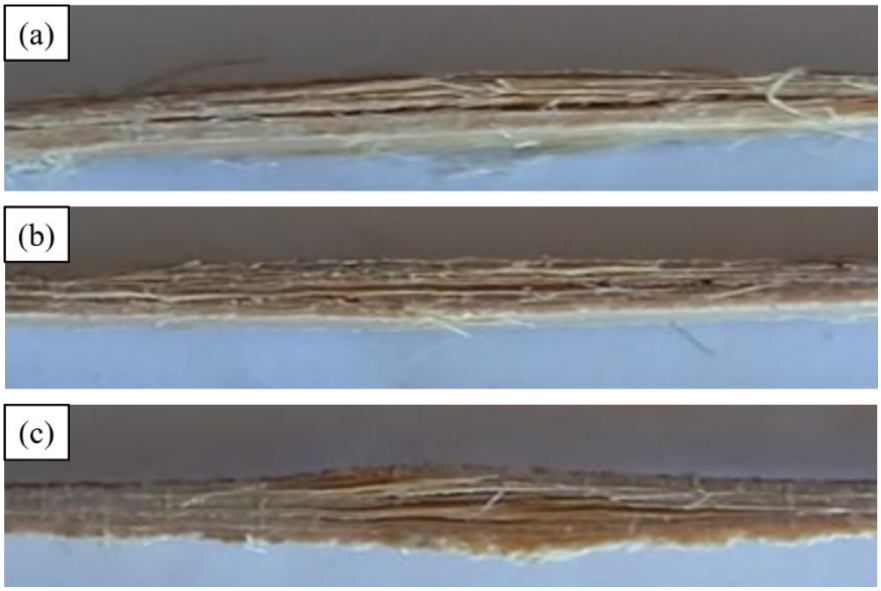

Figure 14 Specimens after tensile test subjected 1344 h of accelerated aging: (a) UD laminate, (b) CP laminate, (c) QI laminate.

From the visual examination of Fig.14a, it can be observed how, for the unidirectional biocomposite, aging gives rise to significant phenomena of fiber-matrix debonding with typical lateral swelling of the specimens; this confirms that the aging process reduces the fiber-matrix adhesion, with associated premature tensile failure of the laminate.

Considering instead the cross-ply (Fig.14b) and the quasi-isotropic (Fig.14c) biocomposite laminates, it is possible to state that the accelerated aging gives rise not only to debonding phenomena, but also to a significant growth of the interlaminar delamination phenomena already, present in unaged laminates (virgin material).

Further investigations through non-destructive investigations on the damage mechanisms were carried out with tomographic methods, a method that in principle allows a better correlation between the extension of the delamination with the progressive aging of the material.

The following Fig.15 shows the tomography acquired from the failured tensile specimens (previously exposed to 1344 *h* of accelerated aging).

From Fig.15 t is easy to see that the three types of specimens (UD, CP and QI) examined, are all visibly more damaged on the upper side directly exposed to the accelerated aging.

In detail, the tomography of the UD laminates, show also extensive delamination phenomena with evident associated phenomena of fiber-bridging involving the of the fibers misaligned with the load. As expected, more evident and widespread delamination phenomena are observed mainly for the CP and QI laminate than for the UD laminate.

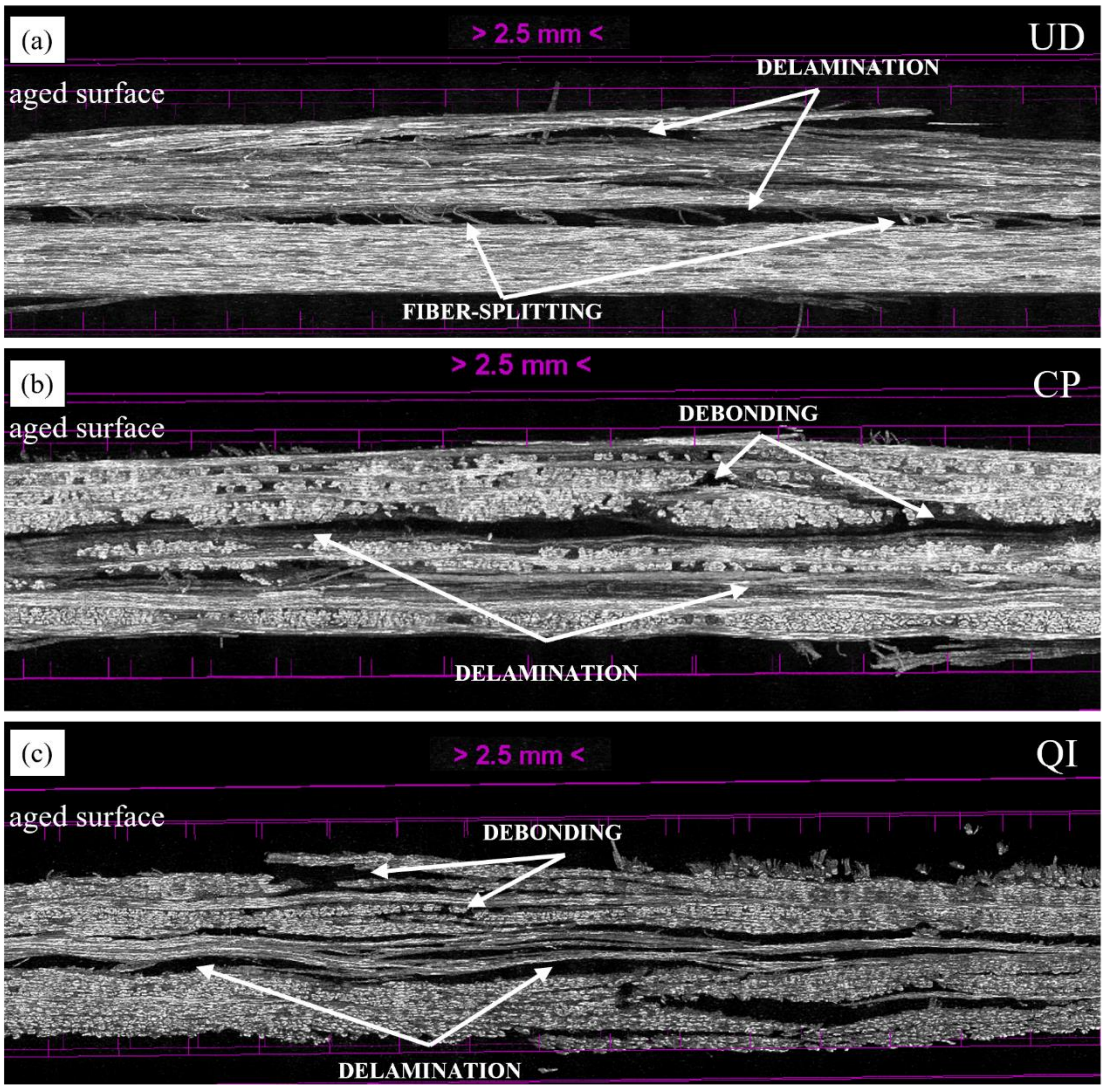

Figure 15 X-ray tomography of the specimens failured by tensile test performed after 1344 h of accelerated aging: (a) UD laminate, (b) CP laminate, (c) QI laminate.

Finally, the following Fig.16 shows the tomography acquired from the various specimens damaged by the delamination tests (ILSS). In detail, the tomography of the unaged specimens (first column), are reported along with those completely aged (1344 *h*) by the two different test configurations, i.e. with aged surface subject to compressive loading (second column) and to tensile loading (third column).

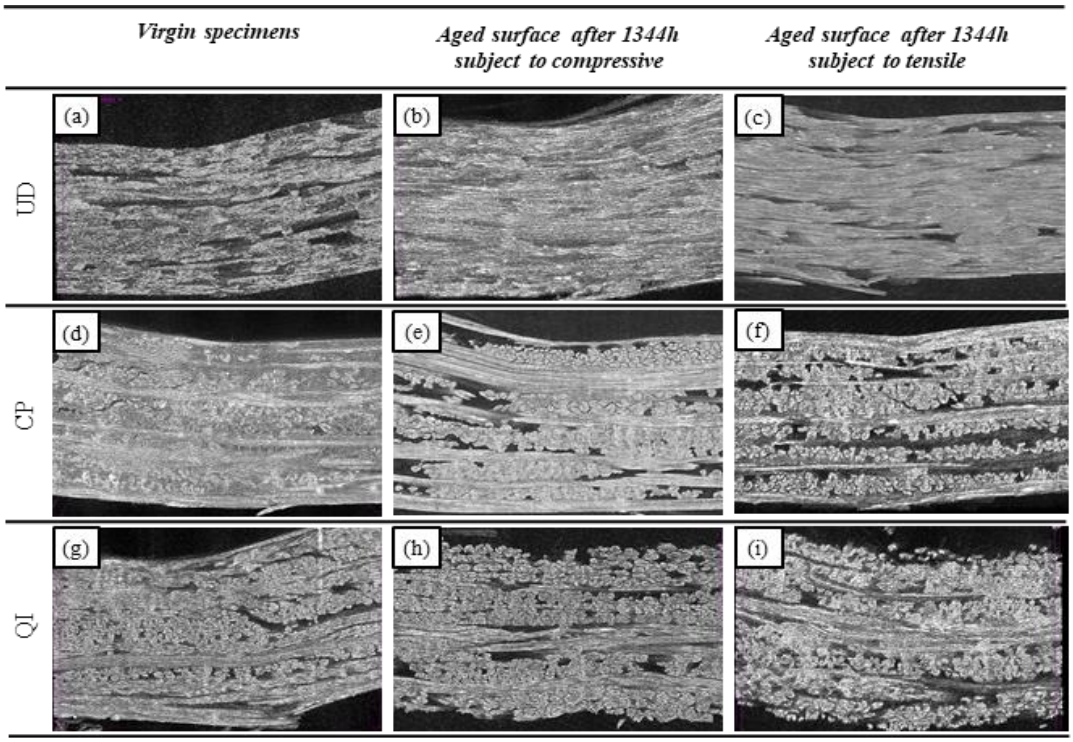

Figure 16 X-ray tomography of the specimens failured by ILSS test.

In this case, x-ray tomography is particularly suitable for the analysis of the internal damage as, due to the small size of the specimens, the visual direct examination is rather difficult.

From the images of the first column of Fig.16 (virgin specimens), it is possible to identify mechanisms of delamination mixed with matrix failure. Finally, comparing the images of the second column of Fig.16 (aged surface subject to compressive), with the images of the third column (aged surface subject to tensile), no significant differences are observed in terms of damage mechanisms; in other words, the presence of compressive loading gives rise to premature debonding and delamination phenomena, which lead to failure with lower applied loads, although with the same damage phenomena.

6. CONCLUSIONS

In conclusion, it is possible to state that the mechanical properties of the studied high performance biocomposites, basically constituted by a green epoxy matrix reinforced with optimized long sisal fibers (already developed and characterized with previous works by the same authors), are significantly influenced by the aging caused by environmental agents such as temperature, humidity and UV. In detail, the execution of accelerated weathering tests carried out in accordance with the ASTM G 154 standard, which predict the exposure of the material to appropriate thermal and UV cycles mixed with humidification cycles, has allowed to detect that both the tensile strength and the delamination strength of unidirectional, cross-ply and quasi-isotropic biocomposite laminates, are significantly influenced by the aging due to the environmental agents.

In particular, it is relieved that the accelerated aging leads to a progressive reduction of the tensile strength with an asymptotical decrement of about 34%-40% after about 8 weeks (1344 h) of exposure. These values are in practice comparable with those previously detected for the neat matrix, so that it is possible to state that in the high performance biocomposites examined, the presence of the sisal fibres does not lead to a significant increase of the environmental degradation. In more details, comparing the results obtained for the different laminates, it was found that the best performances are exhibited by the quasi-isotropic laminates (strength reduction of about -34%), followed by cross-ply (-35%), and unidirectional (-40%). In terms of average stiffness, the accelerated aging leads to comparable reductions, since the failure strain of the different biocomposites remains almost unchanged with aging. The analysis of the experimental results has shown that the degradation of strength and stiffness with the time of aging is well described by a simple exponential relationship univocally defined by three parameters: the properties of the virgin material, of the same material completely aged (subjected in practice to 8 weeks of accelerated aging) and of the *k* exponent related to the material and the particular environmental conditions.

In more details, the knowledge of the response of the examined biocomposite laminate to the accelerated aging allows also to obtain the analytical function that describe the aging process due to an actual working condition by carried out a simple calibration at an arbitrary time *t**. Such a function can be advantageously used at the design stage to predict the evolution of aging as well as the time after which the laminate reaches asymptotically its minimum performance (maximum aging).

Considering instead the strength to delamination, assessed through ILSS tests according to the ASTM D2344 standard, the experimental analysis has shown that the aging due to environmental agents, gives to the lower effects for the quasi-isotropic laminates (QI) that show a maximum delamination strength reduction of 50%, against the value of 70% relieved for the cross-ply (CP) and unidirectional (UD) laminates. Delamination tests carried out by subjecting the surface exposed to the environmental agents to tensile and compressive stresses, also allowed to highlight that the condition with compressive stresses gives rise to further aging effects with delamination strength reduction ranging from 25% to 40% by passing from QI laminates to CP laminates to UD laminates. This is due to the lower compressive strength of the aged material due to the presence of failure related to the transverse tensile, strongly influenced by the degradation of the matrix.

In the presence of prevailing bending loading, the configuration with the surface of the biocomposite laminate subjected to tensile stresses is therefore to be recommended, if severe environmental conditions are present. Although further studies are needed for a detailed analysis of the specific effects of each environmental agent (temperature, UV etc.), the study carried out allows to state that the use of the high-performance biocomposites

analysed, especially in harsh environmental conditions, gives rise to significant aging effects on the mechanical performance, so that fiber treatments to limit hydrophilicity and improve fiber-matrix adhesion, or the use of special surface gel-coats or paints, or the use of surface hybridization with non-hydrophilic fibers such as basalt, are strongly recommended. Such actions are particularly important if the service loading can lead to appreciable delamination phenomena.

Authors contribution

Carmelo Militello: Conceptualization, Methodology, Investigation, Formal analysis, Data Curation, Validation, Writing - Original Draft. **Francesco Bongiorno:** Conceptualization, Methodology, Investigation, Formal analysis, Data Curation, Visualization, Writing - Original Draft. **Bernardo Zuccarello:** Conceptualization, Methodology, Formal analysis, Supervision, Validation, Writing - Review & Editing.

Acknowledgments

The authors gratefully acknowledge the support provided by University of Palermo.

Declaration of competing interest

The authors declare that they have no known competing financial interests or personal relationships that could have appeared to influence the work reported in this paper.

References

[1] Koronis G, Silva A, Fontul M. Green composites: A review of adequate materials for automotive applications. Composites Part B: Engineering 2013;44:120–7. https://doi.org/10.1016/j.compositesb.2012.07.004.

[2] Dittenber DB, Gangarao HVS. Critical review of recent publications on use of natural composites in infrastructure. Composites Part A: Applied Science and Manufacturing 2012;43:1419–29. https://doi.org/10.1016/j.compositesa.2011.11.019.

[3] Azwa ZN, Yousif BF, Manalo AC, Karunasena W. A review on the degradability of polymeric composites based on natural fibres. Materials and Design 2013;47:424–42. https://doi.org/10.1016/j.matdes.2012.11.025.

[4] Summerscales J, Dissanayake N, Virk A, Hall W. A review of bast fibres and their composites. Part 2 - Composites. Composites Part A: Applied Science and Manufacturing 2010;41:1336–44. https://doi.org/10.1016/j.compositesa.2010.05.020.

[5] Le Duigou A, Davies P, Baley C. Exploring durability of interfaces in flax fibre/epoxy micro-composites.

Composites Part A: Applied Science and Manufacturing 2013;48:121–8. https://doi.org/10.1016/j.compositesa.2013.01.010.

[6] Böer P, Holliday L, Kang THK. Independent environmental effects on durability of fiber-reinforced polymer wraps in civil applications: A review. Construction and Building Materials 2013;48:360–70. https://doi.org/10.1016/j.conbuildmat.2013.06.077.

[7] Yorseng K, Rangappa SM, Pulikkalparambil H, Siengchin S, Parameswaranpillai J. Accelerated weathering studies of kenaf/sisal fiber fabric reinforced fully biobased hybrid bioepoxy composites for semi-structural applications: Morphology, thermo-mechanical, water absorption behavior and surface hydrophobicity. Construction and Building Materials 2020;235:117464. https://doi.org/10.1016/j.conbuildmat.2019.117464.

[8] Mukhopadhyay S, Srikanta R. Effect of ageing of sisal fibres on properties of sisal - Polypropylene composites. Polymer Degradation and Stability 2008;93:2048–51. https://doi.org/10.1016/j.polymdegradstab.2008.02.018.

[9] Moudood A, Rahman A, Khanlou HM, Hall W, Öchsner A, Francucci G. Environmental effects on the durability and the mechanical performance of flax fiber/bio-epoxy composites. Composites Part B: Engineering 2019;171:284–93. https://doi.org/10.1016/j.compositesb.2019.05.032.

[10] Bazan P, Mierzwinski D, Bogucki R, Kuciel S. Bio-Based Polyethylene Composites with Natural Fiber: Mechanical, Thermal, and Ageing Properties Patrycja. Materials MDPI 2020;13:2595. https://doi.org/10.3390/ma13112595.

[11] Sodoke FK, Toubal L, Laperrière L. Wetting/drying cyclic effects on mechanical and physicochemical properties of quasi-isotopic flax/epoxy composites. Polymer Degradation and Stability 2019;161:121–30. https://doi.org/10.1016/j.polymdegradstab.2019.01.014.

[12] Pratheep Kumar A, Singh RP, Sarwade BD. Degradability of composites, prepared from ethylene-propylene copolymer and jute fiber under accelerated aging and biotic environments. Materials Chemistry and Physics 2005;92:458–69. https://doi.org/10.1016/j.matchemphys.2005.01.027.

[13] Bajwa DS, Bajwa SG, Holt GA. Impact of biofibers and coupling agents on the weathering characteristics of composites. Polymer Degradation and Stability 2015;120:212–9. https://doi.org/10.1016/j.polymdegradstab.2015.06.015.

[14] Lu T, Solis-Ramos E, Yi YB, Kumosa M. Synergistic environmental degradation of glass reinforced polymer composites. Polymer Degradation and Stability 2016;131:1–8. https://doi.org/10.1016/j.polymdegradstab.2016.06.025.

[15] Lu T, Solis-Ramos E, Yi YB, Kumosa M. Particle removal mechanisms in synergistic aging of polymers and glass reinforced polymer composites under combined UV and water. Composites Science and Technology 2017;153:273–81. https://doi.org/10.1016/j.compscitech.2017.10.028.

[16] Lu T, Solis-Ramos E, Yi Y, Kumosa M. UV degradation model for polymers and polymer matrix composites. Polymer Degradation and Stability 2018;154:203–10. https://doi.org/10.1016/j.polymdegradstab.2018.06.004.

[17] An Z, Xu Z, Ye Y, Yang R. A rapid and highly sensitive evaluation of polymer composite aging with linear correlation to real-time aging. Analytica Chimica Acta 2021;1169:338632. https://doi.org/10.1016/j.aca.2021.338632.

[18] Zuccarello B, Marannano G. Random short sisal fiber biocomposites: Optimal manufacturing process and reliable theoretical models. Materials and Design 2018;149:87–100. https://doi.org/10.1016/j.matdes.2018.03.070.

[19] Zuccarello B, Marannano G, Mancino A. Optimal manufacturing and mechanical characterization of high performance biocomposites reinforced by sisal fibers. Composite Structures 2018;194:575–83. https://doi.org/10.1016/j.compstruct.2018.04.007.

[20] Militello C, Bongiorno F, Epasto G, Zuccarello B. Low-velocity impact behaviour of green epoxy biocomposite laminates reinforced by sisal fibers. Composite Structures 2020;253:112744. https://doi.org/10.1016/j.compstruct.2020.112744.

[21] Zuccarello B, Militello C, Bongiorno F. Influence of the anisotropy of sisal fibers on the mechanical properties of high performance unidirectional biocomposite lamina and micromechanical models. Composites Part A: Applied Science and Manufacturing 2021;143:106320. https://doi.org/https://doi.org/10.1016/j.compositesa.2021.106320 Received.

[22] Zuccarello B, Bartoli M, Bongiorno F, Militello C, Tagliaferro A, Pantano A. New concept in bioderived composites: Biochar as toughening agent for improving performances and durability of agave-based epoxy biocomposites. Polymers 2021;13:1–14. https://doi.org/10.3390/polym13020198.

[23] Bongiorno F, Militello C, Zuccarello B. Mode I translaminar fracture toughness of high performance laminated biocomposites reinforced by sisal fibers: Accurate measurement approach and lay-up effects. Composites Science and Technology 2022;217:109089. https://doi.org/10.1016/j.compscitech.2021.109089.

[24] Pantano A, Militello C, Bongiorno F, Zuccarello B. Analysis of the parameters affecting the stiffness of short sisal fiber biocomposites manufactured by compression-molding. Polymers 2022;14. https://doi.org/10.3390/polym14010154.

[25] Zuccarello B, Bongiorno F, Militello C. Basalt Fiber Hybridization Effects on High-Performance Sisal-Reinforced Biocomposites. Polymer 2022;14:16. https://doi.org/https://doi.org/10.3390/ polym14071457.

[26] Pantano A, Zuccarello B. Numerical model for the characterization of biocomposites reinforced by sisal fibres. Procedia Structural Integrity 2018;8:517–25. https://doi.org/10.1016/j.prostr.2017.12.051.

[27] Zuccarello B, Scaffaro R. Experimental analysis and micromechanical models of high performance renewable agave reinforced biocomposites. Composites Part B: Engineering 2017;119:141–52. https://doi.org/10.1016/j.compositesb.2017.03.056.

[28] Zuccarello B, Zingales M. Toward high performance renewable agave reinforced biocomposites: Optimization of fiber performance and fiber-matrix adhesion analysis. Composites Part B: Engineering 2017;122:109–20. https://doi.org/10.1016/j.compositesb.2017.04.011.

[29] Mancinoa A, Marannano G, Zuccarello B. Implementation of eco-sustainable biocomposite materials reinforced by optimized agave fibers. Procedia Structural Integrity 2018;8:526–38. https://doi.org/10.1016/j.prostr.2017.12.052.

[30] Zuccarello B. Static and dynamic mechanical properties of eco-friendly polymer composites. In: Inamuddin, Thomas S, Kumar Mishra R, Asiri A, editors. Sustainable Polymer Composites and Nanocomposites Springer Nature, Springer, Cham; 2019, p. 259–92. https://doi.org/10.1007/978-3-030-05399-4_9.

[31] Pantano A, Bongiorno F, Marannano G, Zuccarello B. Enhancement of Static and Fatigue Strength of Short Sisal Fiber Biocomposites by Low Fraction Nanotubes. Applied Composite Materials 2021;28:91–112. https://doi.org/10.1007/s10443-020-09857-9.

[32] ASTM G154-06 Standard Practice for Operating Fluorescent Light Apparatus for UV Exposure of Nonmetallic Materials. 2006.

[33] ASTM D3039 Standard Test Method for Tensile Properties of Polymer Matrix Composite Materials. 2002.

[34] ASTM D2344 Standard Test Method for Short-Beam Strength of Polymer Matrix Composite Materials and Their Laminates. 2000.